

Examination of observation and model error for all-sky infrared radiance assimilation



Kozo Okamoto and Masahiro Hayashi (JMA/MRI)

1. Background and purpose

- ✓ Characterizing and modeling of cloud dependent observation error covariances are crucial to all-sky radiance (ASR) assimilation.
- ✓ In order to predict O-B variability (and bias) according to cloud situation, we developed a symmetric cloud effect parameter (Ca) (Okamoto et al. 2014, QJRMS).
- ✓ The Ca functioned well for Metop/IASI and Himawari-8/AHI water vapor (WV) bands when it came to predicting the variability. Thus we developed a cloud-dependent observation error model using Ca (Okamoto 2017; Okamoto et al. 2019).
- ✓ Cloud dependent observation error correlation and treatment for O-B bias are challenges. We are examining their characteristics and cause of biases, and testing some approaches to treat them.

2. Cloud effect parameter (Ca) and (diagonal) observation error model

- ✓ A symmetric cloud effect parameter Ca is defined with
 - ✓ $Ca = \frac{1}{2}\{|O-B_{clear}|+|B-B_{clear}|\}$
 - ✓ O: observation brightness temperature (BT), B: simulated BT, B_{clear} : simulated BT without cloud scattering calculation
- ✓ O-B standard deviation (SD) monotonically increased with Ca and saturated (Figs. 2-1, 2-2). This simple relationship allowed us to predict O-B SD with Ca.
- ✓ O-B normalized by O-B SD from the relationship with Ca showed a Gaussian form (Fig. 2-3).
- ✓ We employed the linear relationship of O-B SD and Ca for a cloud-dependent observation error model. This resulted in cloud-dependent QC, by rejecting samples with O-B over 3 times the observation error.
 - ✓ An examples of observation error after QC is shown in Fig. 2-4.
- ✓ Assimilating ASR of single WV band (band9; 6.9um) of AHI in regional data assimilation system (RDAS) improved first-guess fit to RAOB and precipitation forecast over the clear-sky radiance (CSR) assimilation (Okamoto et al. 2019; QJRMS)
- ✓ Assimilating ASR of AHI in the global data assimilation system (GDAS) is being developed where similar approaches (QC and observation error model) are incorporated. However additional treatment is necessary because GDAS is supposed to assimilate 3 WV bands and suffers from significant underestimation of high clouds in global forecast model (see Section 5)

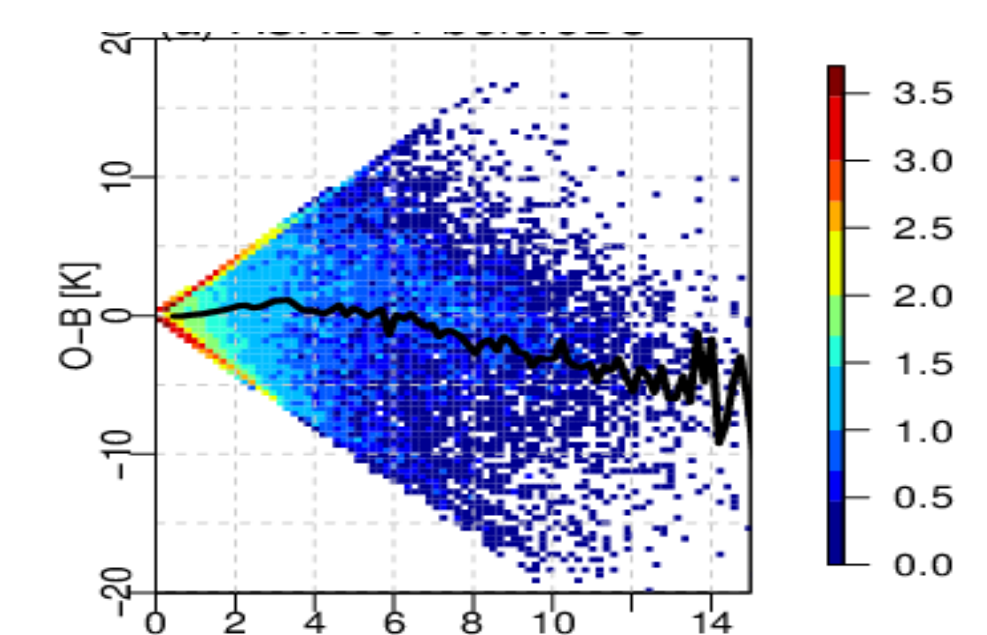


Fig.2-1: Density scatter plot of Ca [K] and O-B [K] at AHI band 9 (6.9um). Black line is a O-B mean at each Ca bin.

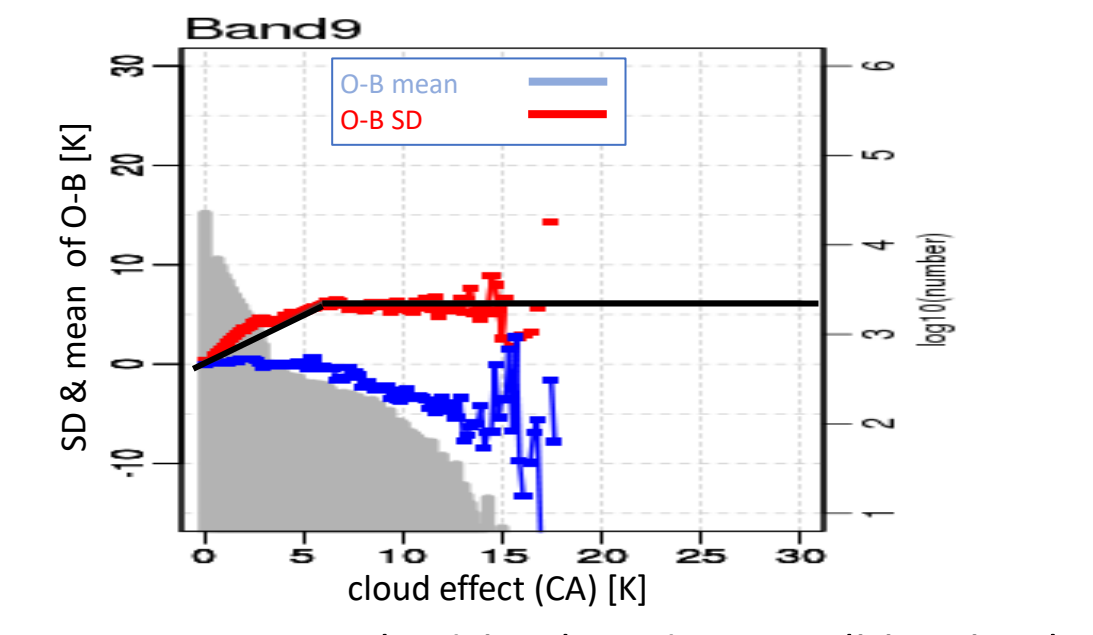


Fig.2-2: O-B SD (red line) and mean (blue line) at AHI band 9, and sample number (grey bars) at each Ca bin. Black line is a linear function to represent O-B-SD with Ca.

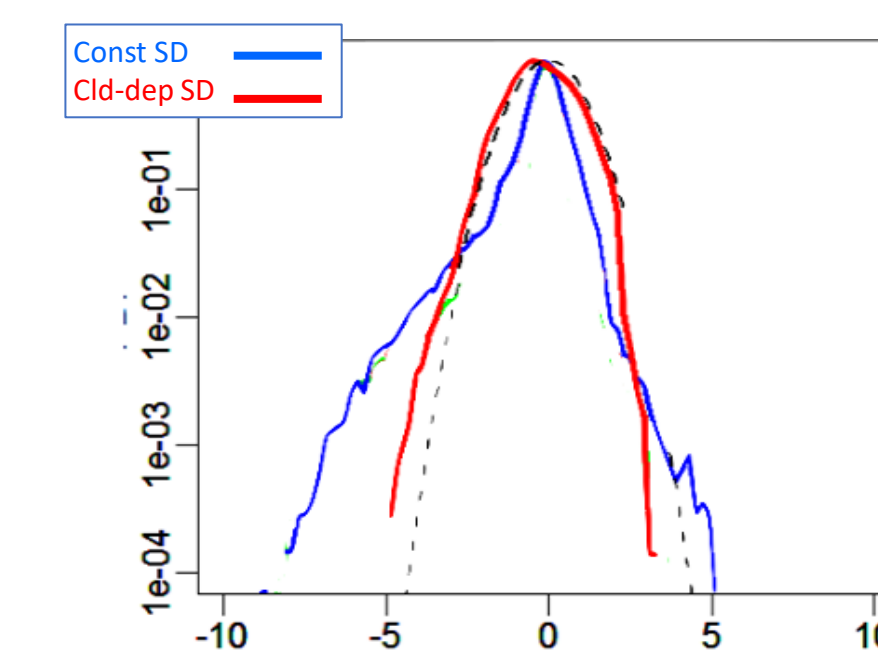


Fig.2-3: PDFs of O-B normalized by O-B SD at AHI band 9. O-B SD is calculated from the whole sample (blue) and from the linear function of Ca in Fig. 2-2 (red). Black dashed line is a normal Gaussian PDF.

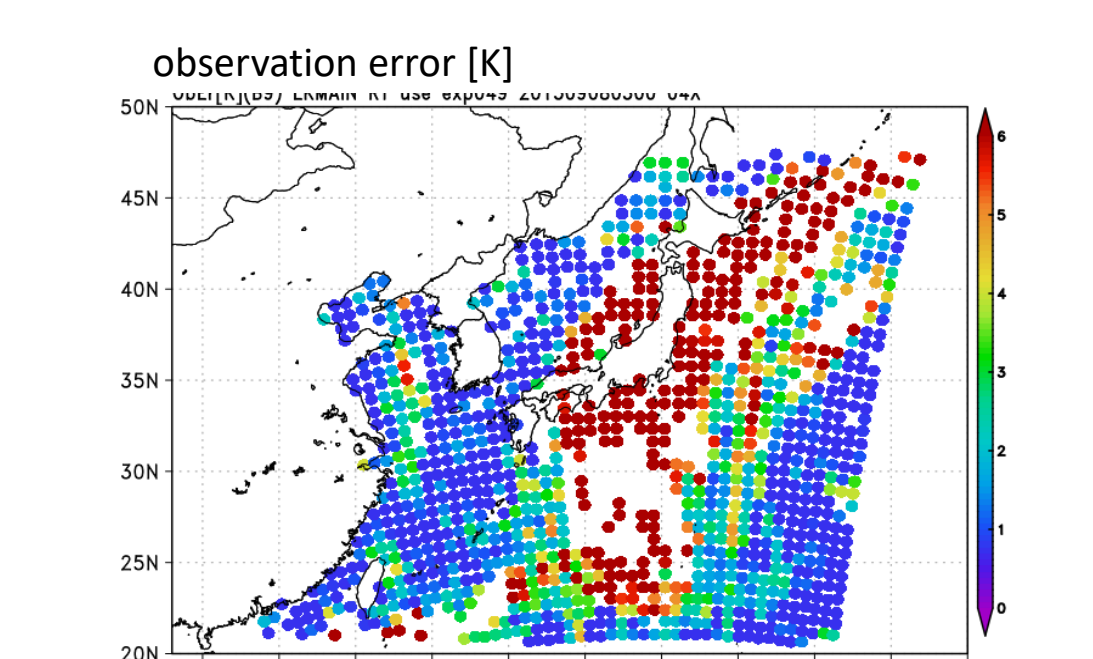


Fig.2-4: observation error [K] of AHI band9 (6.9um) at 03UTC 8 Sep 2015 in RDAS

3. Observation error correlation

- ✓ Spatial and inter-band observation error correlation was examined with Desroziers diagnosis for three WV bands of AHI. The correlation increased with cloud effect.
- ✓ The distance at no correlation (<0.2) was 180 (45) km for band 9 in cloudy (clear-sky or less cloudy) conditions (Fig.3-1 (a, b)). Thus, we thinned ASR data to 75 km (and inflated observation error) in RDAS and to 220 km in GDAS.
- ✓ The correlation of adjacent bands was about 0.8 (0.3) in cloudy (clear-sky or less cloudy) conditions (Fig.3-1 (c, d)). This suggests the need to incorporate cloud-dependent inter-band correlation to assimilate multiple bands.
 - ✓ Ishibashi (in prep): Construct stratified observation error covariances according to cloud effect
 - ✓ Geer (2019, AMT): Scale eigenvalues of eigenvalue decomposed observation error covariances according to cloud effect

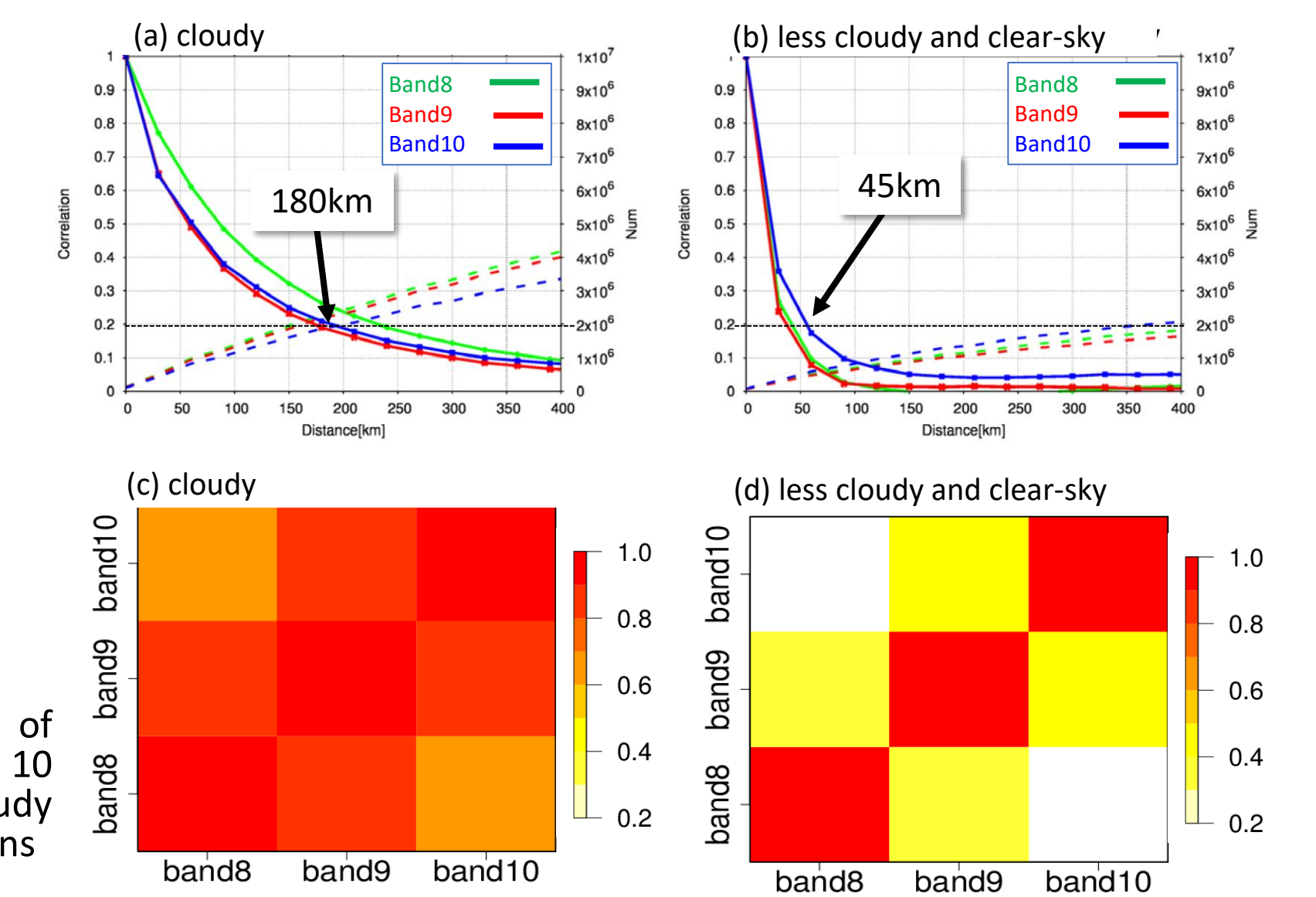


Fig.3-1: (a,b) Spatial and (c,d) Inter-band correlation of observation error at bands 8 (6.2um), 9 (6.9um) and 10 (7.3um) of AHI estimated from samples in (a, c) cloudy (Ca>0.5) and (b, d) less cloudy or clear-sky (Ca<0.5) conditions

4. Examination of O-B bias and correction

- ✓ O-B PDF was examined using RTTOV12.2 simulation using
 - ✓ [DARDAR] accurate ice cloud profile product from CALIPSO-CLOUDSAT (Dalanoe J. and R. J. Hogan, 2010, JGR), and
 - ✓ [GSM] JMA's operational global model when cloud top height and fraction were consistent with observation
- ✓ Negative O-B bias was obvious especially at low observed BT for GSM (Fig.4-1 (b, d)) although it was not clear for DARDAR (Fig.4-1 (a, c)). This suggests significant underestimation of high cloud in forecast model. (model cloud bias)
- ✓ Positive O-B bias was also found in thin cloud for both DARDAR and GSM (Fig. 4-1), probably due to the overestimated ice cloud absorption of RTTOV. (RTM cloud bias)
- ✓ The JMA's global model has dry bias in the middle troposphere, leading to negative O-B bias in AHI bands 9 and 10 (not shown here). (model WV bias)

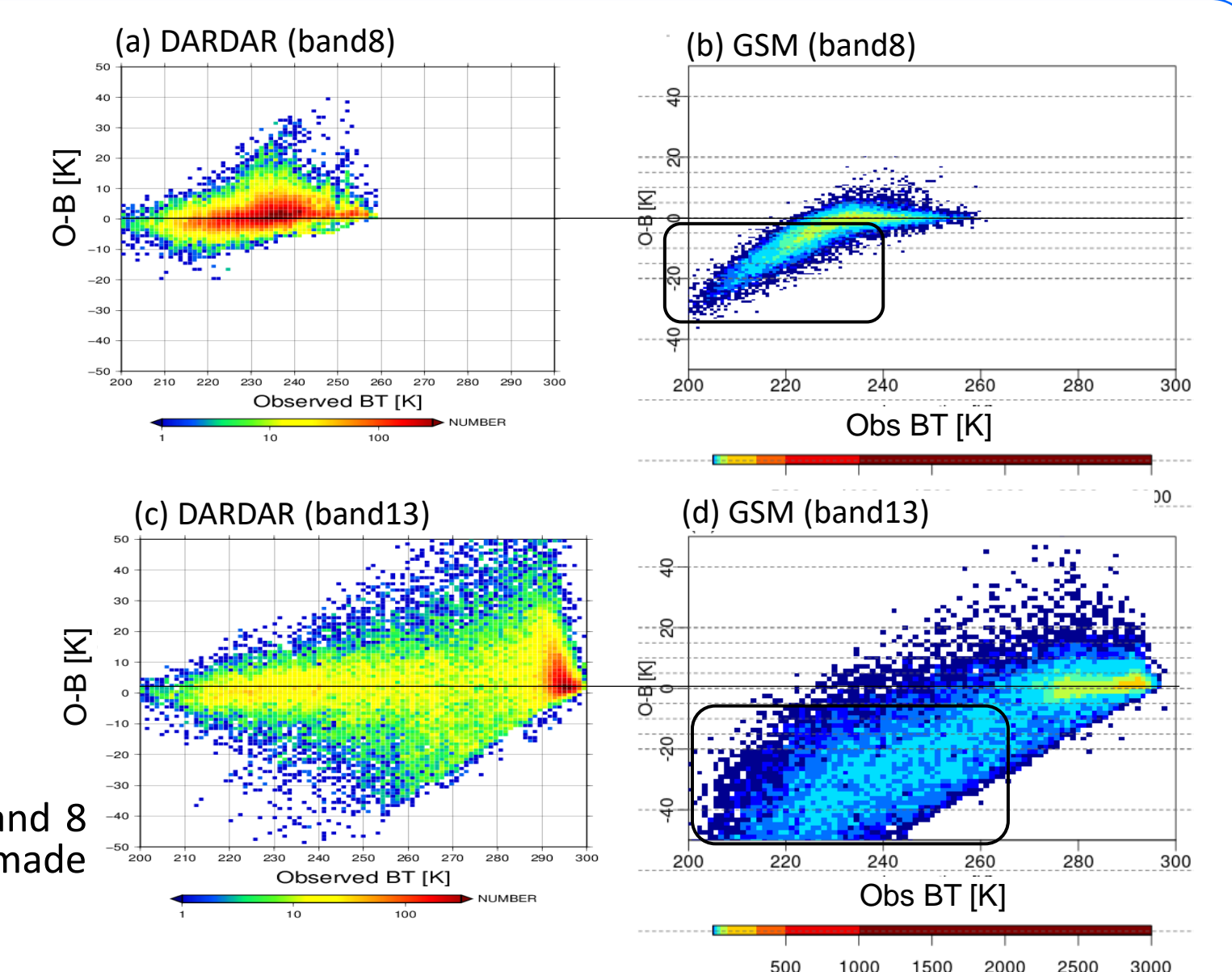


Fig.4-1: Density scatter plot of observed BT and O-B at AHI (a, b) band 8 (6.2um) and (c, d) band 13 (10.2um). The radiance simulation was made from ice cloud profiles of (a,c) DARDAR and (b,d) GSM.

5. Trial bias correction (BC)

- ✓ In the RDAS, we tested two BC approaches with
 - ✓ BC1: Used the same predictors as CSR assimilation and estimated BC coefficients from less cloudy samples only: $bc = a_1 TB_{clr} + a_2 \cos\theta + a_3$
 - ✓ BC2: focused on correcting cloud-induced bias: $bc = a_1 Ca + a_2 Ca^2 + a_3 Ca^3 + a_4$
- ✓ Both BC1 and BC2 experiments gave comparable improvements to experiments without BC although BC themselves performed well as expected (Fig.5-1).
- ✓ We speculate that the reason why BC did not give additional benefit is
 - ✓ BC1 did not treat RTM cloud bias and corrected only WV dependent bias
 - ✓ BC2 corrected model cloud bias for samples with modest to large Ca. These samples were not abundant and their observation errors were highly inflated, which reduced impact of BC
- ✓ These trials suggest that in RDAS the bias is not so much that QC and observation error inflation can suppress bias-induced bad effect.

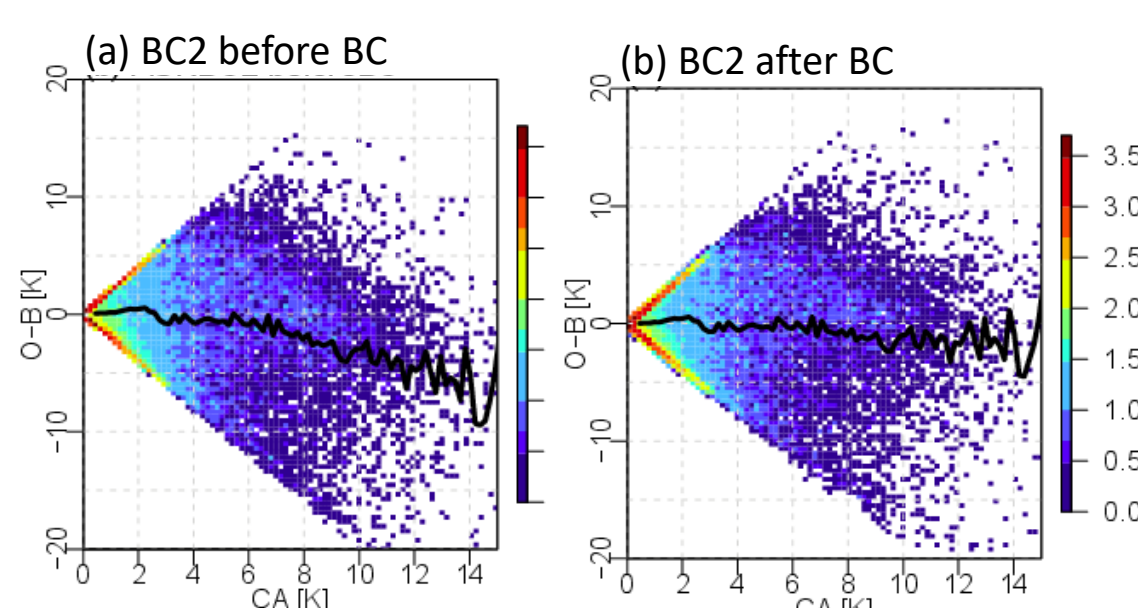


Fig.5-1: Density scatter plot of Ca and O-B at AHI band 9 for (a) before and (b) after BC2 in RDAS. Black lines are mean O-B at each Ca bin.

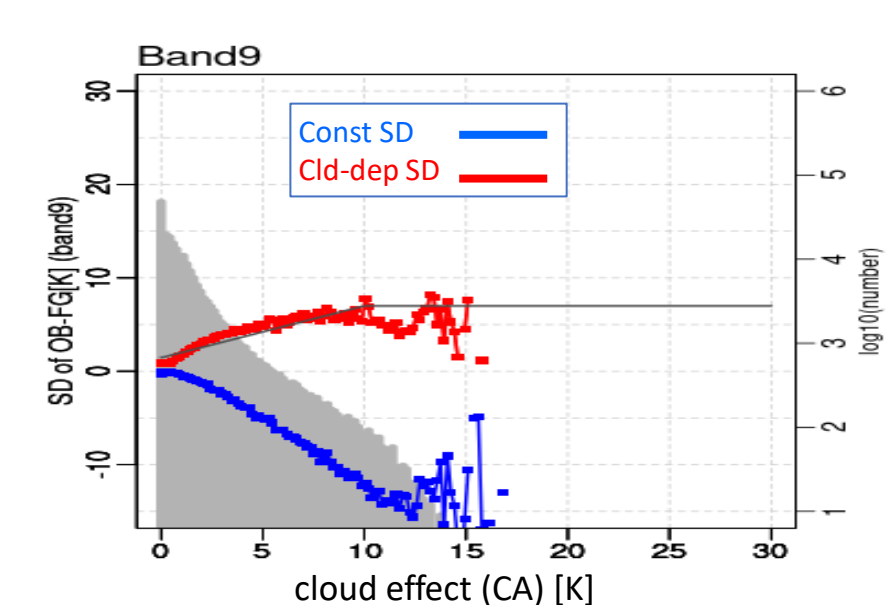


Fig.5-2: The same as Fig.1-2, in GDAS

- ✓ In GDAS, however, larger negative bias was found due to more significant underestimation of high cloud (Fig.5-2). BC may be needed that takes into account the model bias because it seems that bias-induced bad impact cannot be fully compensated by QC and observation error inflation.
- ✓ We are testing cloud-dependent BC for numerous samples with small to medium Ca and further observation inflation for samples with medium and large Ca. This treatment is partially equivalent to Chambon et al. (2010, QJRMS) in that the former samples have similar cloud effect in observations and model.
- ✓ Other challenges:
 - ✓ How to distinguish the RTM and model biases and correct RTM bias (and model bias)?
 - ✓ If model bias correction is necessary, how much model bias should be corrected?
 - ✓ The significant model bias might violate symmetry in Ca because model cloud effect tends to be underestimated in Ca.
 - ✓ This may be handled by BCed Ca and modified observation error model (e.g. Lonitz and Geer 2020)

6. Conclusion

- ✓ We developed a symmetric cloud effect parameter Ca for all-sky IR radiance assimilation to effectively predict O-B variability and created a cloud dependent (diagonal) observation error model.
- ✓ Inter-band correlation increases with the cloud effect and needs to be incorporated in DAS when assimilating multiple channels.
- ✓ Detrimental impacts of bias can be alleviated by adequate QC and observation error inflation without BC, as in experiment in RDAS.
- ✓ However, BC and additional treatments may be necessary if the bias is beyond the tolerance level. We are investigating how to handle or correct model bias in GDAS.

References

- ✓ Chambon, P., S. Q. Zhang, A. Y. Hou, M. Zupanski, and S. Cheung, 2014: Assessing the impact of pre - GPM microwave precipitation observations in the Goddard WRF ensemble data assimilation system. *Quart. J. Roy. Meteor. Soc.*, **140**, 1219-1235. doi:10.1002/qj.2215.
- ✓ Dalanoe J. and R. J. Hogan 2010: Combined CloudSat-CALIPSO-MODIS retrievals of the properties of ice clouds. *J. Geophys. Res.*, **115**, D00H29, doi:10.1029/2009JD012346.
- ✓ Geer, A. J. 2019: Correlated observation error models for assimilating all-sky infrared radiances, *Atmos. Meas. Tech.*, **12**, 3629-3657, https://doi.org/10.5194/amt-12-3629-2019.
- ✓ Lonitz, K. and A. J. Geer, 2020: Reducing the drying effect through a water vapour correction to the all-sky error model. *Technical Report 53, EUMETSAT/ECMWF Fellowship Programme Research Report*, doi:10.21957/qmy8utgbg, URL https://www.ecmwf.int/node/19528.
- ✓ Okamoto, K., T. McNally and W. Bell, 2014: Progress towards the assimilation of all-sky infrared radiances: an evaluation of cloud effects. *Quart. J. Roy. Meteor. Soc.*, **140**, 1603-1614, doi: 10.1002/qj.2242.
- ✓ Okamoto, K. 2017: Evaluation of IR radiance simulation for all-sky assimilation of Himawari-8/AHI in a mesoscale NWP system. *Quart. J. Roy. Meteor. Soc.*, **143**, 1517-1527. doi:10.1002/qj.3022.
- ✓ Okamoto, K., Y. Sawada and M. Kunii, 2019: Comparison of assimilating all - sky and clear - sky infrared radiances from Himawari-8 in a mesoscale system. *Quart. J. Roy. Meteor. Soc.* **145**, 745- 766. doi.org/10.1002/qj.3463.